Available online at www.sciencedirect.com

ScienceDirect

Ceramics International 39 (2013) 8723–8727

CERAMICS INTERNATIONAL

www.elsevier.com/locate/ceramint

Microwave dielectric properties of Al-doped ZnO powders synthesized by coprecipitation method

Yuan Wang*, Fa Luo, Ling Zhang, Dongmei Zhu, Wancheng Zhou

State Key Laboratory of Solidification Processing, Northwestern Polytechnical University, Xi'an 710072, PR China

Received 9 July 2012; received in revised form 16 April 2013; accepted 16 April 2013
Available online 22 April 2013

Abstract

Al-doped ZnO (AZO) powders with different Al concentrations were synthesized by coprecipitation method. Crystal structural and dielectric properties of the powders as a function of aluminum doping concentration as well as annealing temperature were investigated. The XRD results reveal that Al atoms are doped into ZnO lattice successfully and all the samples are polycrystalline with a hexagonal wurtzite structure. The real part (ε') and imaginary part (ε'') of the complex permittivity of the powders were carried out by a vector network analyzer in the microwave frequency range of 8.2–12.4 GHz. The results show that the ε' and ε'' of the doped ZnO powders increase with the doping content and both of them are higher than that of the pure one. For the AZO powder with 7 mol% Al, both ε' and ε'' increase firstly and then decrease with increasing annealing temperature.

Keywords: D. ZnO; Aluminum; AZO; Doping; Permittivity

1. Introduction

Much attention has been paid to ZnO in recent years due to its broad applications in UV light-emitters, varistors, transparent high power electronics, gas-sensing and as a window material for display and solar cells [1–4]. Doping with other elements can greatly improve the performance of ZnO [5–13]. Among these doped ZnO materials, aluminum doped ZnO (AZO) films have received considerable attention [14–18] because they not only exhibit excellent optical and electrical properties which are comparable to those of ITO film [19,20], but also have the advantage of abundant and cheap raw materials. However, the application range of AZO materials has been limited by the limitation of film characteristics.

As the complementation of AZO film material, the AZO powders show a great power in many applications such as photocatalyst [21–23], ethanol gas sensor [24], transmitter [22,25–27], sterilizer [28] and the AZO sputtering target [29]. Furthermore, they can be used as functional filler for anti-static coatings [30] or microwave absorbing coatings [22,31,32]. Great efforts have been made to research the preparation methods and relevant properties. Unfortunately, the research on the dielectric properties which has a fundamental effect on its applications in industrial, commercial and military fields is still lacking. According to the theoretical calculation made by Huang et al. [33], both the ε' and ε'' of the doped ZnO powders are higher than those of undoped one. Al-doped ZnO/$ZrSiO_4$ composite ceramics have been made by Kong et al. [32]. They found that both dielectric loss and microwave absorption properties of the composite ceramics are affected by the Al content. However, to the best of our knowledge no report has been reported on the effect of annealing temperature on the dielectric properties of AZO powders, which is crucial for its potential applications at high temperature.

In this paper, the ZnO powders doped with Al were synthesized by coprecipitation method and the effects of Al-doped concentration and annealing temperature on the dielectric properties of AZO powders were investigated to provide some useful guides to the high temperature application of this material.

2. Experimental

2.1. Sample preparation

Pure and Al-doped ZnO powders were synthesized by coprecipitation method and $Zn(NO_3)_2 \cdot 6H_2O$, $Al(NO_3)_3 \cdot 9H_2O$

*Corresponding author. Tel./fax: +86 029 88494574.
E-mail addresses: yccd425@yahoo.cn, wangyuan20080808@163.com (Y. Wang).

0272-8842/$ - see front matter © 2013 Elsevier Ltd and Techna Group S.r.l. All rights reserved.
http://dx.doi.org/10.1016/j.ceramint.2013.04.056

and $CO(NH_2)_2$ were used as starting material, dopant and precipitator, respectively. All the chemical reagents were analytical grades and used without further purification.

Firstly, $Zn(NO_3)_2 \cdot 6H_2O$, $Al(NO_3)_3 \cdot 9H_2O$ and $CO(NH_2)_2$ were separately dissolved in de-ionized water. Secondly, appropriate amounts of $Al(NO_3)_3 \cdot 9H_2O$ solutions were added into the $Zn(NO_3)_2 \cdot 6H_2O$ solution to obtain desired Al-doping concentration. In our study, the Al dopant level was defined by the Al/(Al+Zn) ratio and it varied from 0 to 11 mol%. Finally, $CO(NH_2)_2$ solution was slowly added into these above mixture solutions. The as-prepared solutions were continually stirred at 80 °C for 1 h to yield precipitates. After filteration, the precipitates were washed with distilled water and ethanol several times, dried in air at 120 °C on stove. Pure ZnO and AZO powders were obtained after the precipitates were annealed at 500 °C for 1 h.

The following reactions (1)–(5) took place when the mixed solutions of $Zn(NO_3)_2 \cdot 6H_2O$, $NH_3 \cdot H_2O$ and $Al(NO_3)_3 \cdot 9H_2O$ were heated. The deposition of $ZnCO_3 \cdot 2Zn(OH)_2 \cdot H_2O$ and $Al(OH)(NO_3)_2 \cdot H_2O$ took place synchronously, which contributes to the coprecipitation of $ZnCO_3 \cdot 2Zn(OH)_2 \cdot H_2O$ and $Al(OH)(NO_3)_2 \cdot H_2O$. During the process of annealing, there are four main chemical reactions described by Eqs. (6)–(9). And the Al-doped ZnO crystal is formed as the Eq. (9) shows.

$$CO(NH_2)_2 + 3H_2O \rightarrow CO_2\uparrow + 2NH_3H_2O \quad (1)$$

$$NH_3H_2O \rightarrow NH_4^+ + OH^- \quad (2)$$

$$2NH_3\ H_2O + CO_2 \rightarrow 2NH_4{}^+ + CO_3{}^{2-} \quad (3)$$

$$3Zn^{2+} + CO_3^{2-} + 4OH^- + H_2O \rightarrow ZnCO_3 2Zn(\ OH)\ _2H_2O\downarrow \quad (4)$$

$$Al(NO_3)_3 9H_2O \rightarrow Al(OH)(NO_3)_2H_2O\downarrow + HNO_3 + 7H_2O \quad (5)$$

$$ZnCO_3 2Zn(\ OH)\ _2H_2O \rightarrow 3ZnO + 3H_2O + CO_2\uparrow \quad (6)$$

$$2Al(\ OH)(\ NO\ _3)_2H_2O \rightarrow Al_2O_3 + 2N_2O + 3H_2O \quad (7)$$

$$Al_2O + ZnO \rightarrow ZnAl_2O_4 \quad (8)$$

$$Al_2O_3 \overset{ZnO}{\Longrightarrow} 2Al_{Zn}{}^{\cdot} + 2O_O + 1/2O_2\uparrow + 2e' \quad (9)$$

2.2. Sample characterization

X-ray powder diffraction (XRD, X'Pert MPD PRO) with a Cu-K_α radiation was used to investigate the crystal structures of as-received powders. For the measurements of complex permittivity, the as-received powders were firstly dispersed in molten paraffin wax (the weight ratio of powder to paraffin wax was 80/20), and then the mixtures were molded into a brass flange to fabricate rectangular composite samples (22.86 mm(length) × 10.16 mm (width) × 2 mm(thickness)). The dielectric parameters of the mixtures were determined by a PNA network analyzer (Agilent Technologies E8362B, Palo Alto, CA) using wave-guide technique with mode TE10 in the frequency range of 8.2–12.4 GHz.

3. Results and discussions

3.1. Effect of dopant concentration

It is well known that whether atoms or ions added go into interstitial or substitutional sites mainly depend on the atoms or ions size and valence difference between guest atoms or ions and host ions. The radii of Al^{3+} and Zn^{2+} are 0.51 and 0.74 Å, respectively. [32,34] When Al dissolves in the ZnO lattice, there are two kinds of possible site for Al to occupy. Al atoms may either occupy the sites where Zn atoms would normally be present or enter the interstitial position of ZnO lattice [35,36]. In fact, Al atoms prefer to occupy Zn sites in the form of $Al_{Zn}^{\cdot}$ for two reasons. Firstly, the formation energy of Al atoms occupying the Zn sites (−5.2168 eV/atom) is much lower than that of Al atoms going into the interstitial (−4.7585 eV/atom). [37] Secondly, the interstitial Al would greatly intensify the lattice distortion of the ZnO crystal lattice.

The X-ray diffraction patterns of Al-doped ZnO powders with different Al concentrations are shown in Fig. 1. It can be clearly seen that when the Al concentration ranges from 0 to 7 mol%, the diffraction patterns of the Al-doped ZnO powders are quite identical to the ZnO figure standard card (Card no. 36-1451) and no diffraction peaks of Al_2O_3 or other second-phase inclusions are observed. However, a peak related to $ZnAl_2O_4$ appears when the content of Al is up to 11 mol%. Except for the characteristics mentioned above, the peaks shift is also significant (shown in the inset of Fig. 1). The positions of (100), (002) and (101) diffraction peaks shift to larger angle as the Al content increases from 0 to 11 mol%, indicating that the Al atoms have incorporated into the ZnO lattice and occupied partial Zn sites.

Fig. 2 presents the real part (ε') and imaginary part (ε'') of complex permittivity of the prepared AZO powders annealed at 500 °C in air for 1 h. It can be seen that both the ε' and ε'' of AZO powders show a general decreasing tendency in the measured

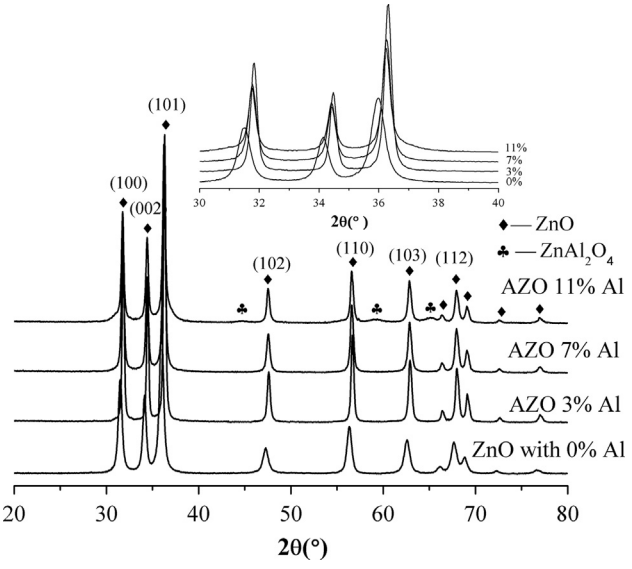

Fig. 1. XRD patterns of AZO with different Al contents.

frequency range, while their absolute values increase significantly with increasing Al doping content and the real part increase less rapidly than the imaginary one. When the doped Al content is up to 11 mol%, the ε' and ε'' of the sample are 4.3–4.0 and 2.6–2.3, respectively, with the maximum values in all samples.

3.2. Effect of annealing temperature

In order to study the effect of annealing temperature on the dielectric properties of AZO powders, the doped powders with 7 mol% Al were annealed at different temperatures (500 °C, 600 °C, 700 °C and 800 °C). Fig. 3 and Table 1 are the XRD patterns and XRD analysis results of the doped powders, respectively. In Fig. 3, it can be observed that the major diffraction peaks match with the standard powder diffraction peaks of ZnO and no diffraction peaks of second-phase inclusions are observed when the annealing temperature is below 600 °C. When the annealing temperature is higher than 700 °C, the peaks of $ZnAl_2O_4$ can be observed and the intensities of the peaks increase with increasing annealing temperature. In addition, as displayed in the inset of Fig. 3, the diffraction angle (2θ) of the peaks first increase and then decrease dramatically with increasing annealing temperature. The diffraction angle of AZO powder annealed at 700 °C is the largest one. This behavior is in good agreement with the XRD analysis results shown in Table 1. It can be explained by the position of Al atoms. As mentioned above, the radius of Zn^{2+} is larger than that of Al^{3+}. When Al atoms occupy Zn sites, the lattice constants decrease due to the different ion radius, which makes the diffraction peaks shift in the direction of higher diffraction angle. However, with increasing annealing temperature, a lot of doping Al atoms that obtained enough thermal activation energy would react with Zn atoms and O atoms, which is demonstrated by the formation of $ZnAl_2O_4$. The amount of substitutional Al is reduced, which leads to the increase of interlayer spacing. According to the Bragg formula, the diffraction peaks shift to lower diffraction angle.

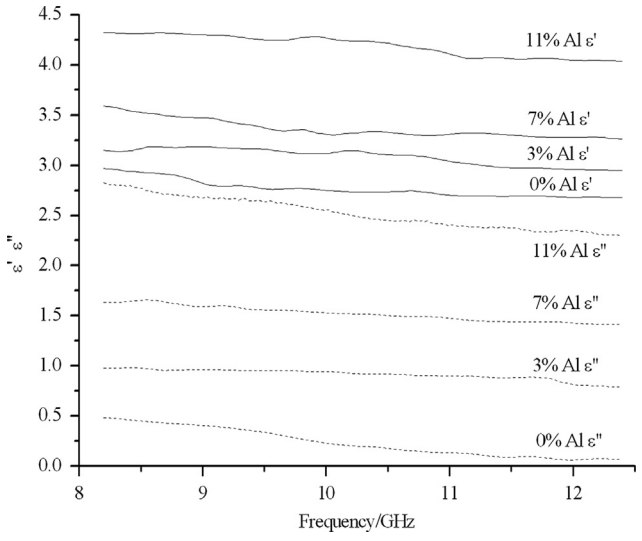

Fig. 2. Real and imaginary parts of the AZO powders with different Al contents.

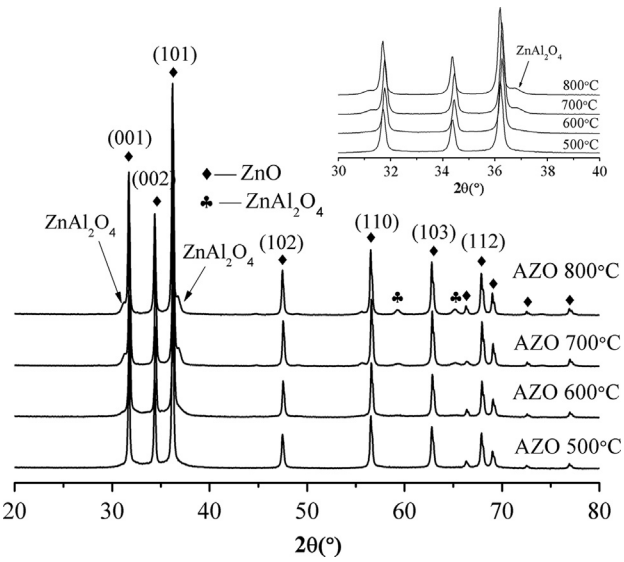

Fig. 3. XRD patterns of AZO powders with 7 mol% Al annealed at different temperatures.

Table 1
The XRD analysis results of the Al-doped ZnO powder annealed at different temperatures.

Annealing temperature (°C)	2θ (°)			d (nm)		
	(100)	(002)	(101)	(100)	(002)	(101)
500	31.708	34.354	36.194	0.28196	0.26083	0.24797
600	31.774	34.421	36.260	0.28139	0.26033	0.24754
700	31.775	34.443	36.261	0.28138	0.26017	0.24753
800	31.702	34.353	36.189	0.28201	0.26083	0.24801

From Table 1, it can be observed that when the annealing temperature is below 700 °C, the interlayer spacing decreases with increasing annealing temperature, which indicates that the amount of substitutional Al increases during the annealing process. In addition, both the diffraction angle and interlayer spacing of the powder annealed at 600 °C are similar to those of the powder annealed at 700 °C. This means that the substitution of Zn with Al has reached the saturation point, which can be further demonstrated by the formation of second phase $ZnAl_2O_4$.

Fig. 4 shows the real and imaginary parts of the permittivity for the 7 mol% Al-doped powder annealed at different temperatures. It can be seen that the values of ε' and ε'' increase firstly and then decrease with increasing annealing temperature. Additionally, the ε' and ε'' of all the AZO powders decrease with increasing frequency. This phenomenon is favorable to the impedance match of microwave absorption properties and increasing the bandwidth. The values of complex permittivity for the sample annealed at 600 °C and 700 °C are very close. The powders annealed at 600 °C and 700 °C have the highest ε'' and ε', respectively. When the annealing temperature is up to 800 °C, both the ε' and ε'' decease rapidly and have the lowest value at all the measured frequencies.

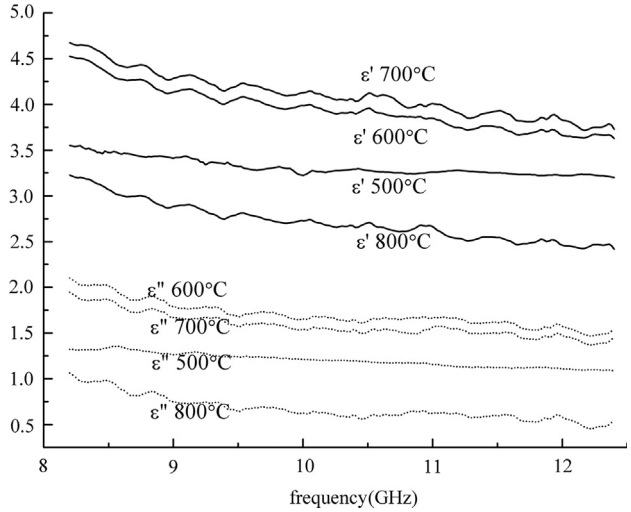

Fig. 4. Complex permittivity as a function of frequency for 7 mol% Al-doped powder annealed at different temperatures.

4. Conclusions

In this study, AZO (Al-doped ZnO) powders prepared by coprecipitation method have been obtained. The effects of aluminum doping concentration and annealing temperature on structural and dielectric properties of the powders were investigated. The results support the following conclusion:

1. The XRD peaks shift to the direction of higher angle with increasing Al concentration. It proves that the prepared powders are solid–solutions where Al atoms enter into the lattice of ZnO at the sites of Zn.
2. Both the ε' and ε'' of AZO powders increase with the increase of Al dopant concentrations.
3. The complex permittivity of the powder is also related to the annealing temperature. For the 7 mol% Al-doped powder, the value of ε' and ε'' are highest when the annealing temperature is 700 °C and 600 °C, respectively. Both the lower and higher annealing temperature can lead to the decrease of complex permittivity.
4. These results are important because they show that changing the doping content or the annealing temperature can significantly affect the dielectric properties of the AZO powders.

Acknowledgments

The authors would like to gratefully acknowledge the other members of our laboratory for their assistance and fruitful discussions. This work has been supported by the National Natural Science Foundation of China (No. 51072165).

References

[1] Ü. Özgür, Ya.I. Alivov, C. Liu, A. Teke, M.A. Reshchikov, S. Doğan, V. Avrutin, S.-J. Cho, H. Morkoç, A comprehensive review of ZnO materials and devices, Journal of Applied Physics 98 (2005) 041301.
[2] Q.H. Li, T. Gao, Y.G. Wang, T.H. Wang, Adsorption and desorption of oxygen probed from ZnO nanowire films by photocurrent measurements, Applied Physics Letters 86 (2005) 123117.
[3] W. Liu, S.L. Gu, J.D. Ye, S.M. Zhu, S.M. Liu, X. Zhou, R. Zhang, Y. Shi, Y.D. Zheng, Blue–yellow ZnO homostructural light-emitting diode realized by metalorganic chemical vapor deposition technique, Applied Physics Letters 88 (2006) 092101.
[4] D.J. Lee, J.Y. Park, Y.S. Yun, Y.S. Hong, J.H. Moon, B.T. Lee, S. S. Kim, Comparative studies on the growth behavior of ZnO nanorods by metalorganic chemical vapor deposition depending on the type of substrates, Journal of Crystal Growth. 276 (2005) 458.
[5] E. Pál, V. Hornok, A. Oszkó, I. Dékány, Hydrothermal synthesis of prism-like and flower-like ZnO and indium-doped ZnO structures, Colloids and Surface A: Physicochemical and Engineering Aspects 340 (2009) 1–9.
[6] P. Palacios, K. Sánchez, P. Wahnón, Ab-initio valence band spectra of Al, In doped ZnO, Thin Solid Films 517 (2009) 2448–2451.
[7] J.P. Wiff, Y. Kinemuchi, H. Kaga, C. Ito, K. Watari, Correlations between thermoelectric properties and effective mass caused by lattice distortion in Al-doped ZnO ceramics, Journal of the European Ceramic Society 29 (2009) 1413–1418.
[8] D. Behera, B.S. Acharya, Study of the microstructural and photoluminescence properties of Li-doped ZnO thin films prepared by spray pyrolysis, Ionics 16 (2010) 543–548.
[9] R. Elilarassi, G. Chandrasekaran., Microstructural and photoluminescence properties of Co-doped ZnO films fabricated using a simple solution growth method, Materials Science in Semiconductor Processing 14 (2011) 179–183.
[10] R. Yousefi, F. Jamali-Sheini, A. Khorsand Zak, M.R. Mahmoudian, Effect of indium concentration on morphology and optical properties of In-doped ZnO nanostructures, Ceramics International 38 (2012) 6295–6301.
[11] S. Lee, D. Cheon, W.J. Kim, M.H. Ham, W. Lee, Ga-doped ZnO films deposited with varying sputtering powers and substrate temperatures by pulsed DC magnetron sputtering and their property improvement potentials, Applied Surface Science 258 (2012) 6537–6544.
[12] C.Y. Tsay, C.W. Wu, C.M. Lei, F.S. Chen, C.K. Lin, Microstructural and optical properties of Ga-doped ZnO semiconductor thin films prepared by sol–gel process, Thin Solid Films 519 (2010) 1516–1520.
[13] S.J. Oh, M.N. Jung, S.Y. Ha, S.G. Choi, J.J. Kim, K. Kobayashi, S.T. Lee, H.C. Lee, Y.R. Cho, T. Yao, J.H. Chang, Microstructure evolution of highly Ga-doped ZnO nanocrystals, Physica E 41 (2008) 31–35.
[14] E. Bacaksiz, S. Aksu, S. Yılmaz, M. Parlak, M. Altunbaş, Structural, optical and electrical properties of Al-doped ZnO microrods prepared by spray pyrolysis, Thin Solid Films 518 (2010) 4076–4080.
[15] Y.S. Kim, W.P. Tai, Electrical and optical properties of Al-doped ZnO thin films by sol–gel process, Applied Surface Science 253 (2007) 4911–4916.
[16] R. Chandramohan, T.A. Vijayan, S. Arumugam, H.B. Ramalingam, V. Dhanasekaran, K. Sundaram, T. Mahalingam, Effect of heat treatment on microstructural and optical properties of CBD grown Al-doped ZnO thin films, Materials Science and Engineering: B 176 (2011) 152–156.
[17] L. Dghoughi, F. Ouachtari, M. Addou, B. Elidrissi, H. Erguig, A. Rmili, A. Bouaoud, The effect of Al-doping on the structural, optical, electrical and cathodoluminescence properties of ZnO thin films prepared by spray pyrolysis, Physica B 405 (2010) 2277–2282.
[18] E.L. Papadopoulou, M. Varda, K. Kouroupis-Agalou, M. Androulidaki, E. Chikoidze, P. Galtier, G. Huyberechts, E. Aperathitis, Undoped and Al-doped ZnO films with tuned properties grown by pulsed laser deposition, Thin Solid Films. 516 (2008) 8141–8145.
[19] K. Yasuia, A. Asanoa, M. Otusjia, H. Katagirib, A. Masudac, H. Nishiyamaa, Y. Inouea, M. Takata, T. Akahane, Improvement of the uniformity in electronic properties of AZO films using an RF magnetron sputtering with a mesh grid electrode, Materials Science and Engineering: B 148 (2008) 26–29.
[20] J.G. Lu, Z.Z. Ye, Y.J. Zeng, L.P. Zhu, L. Wang, J. Yuan, B.H. Zhao, Structural, optical, and electrical properties of (Zn, Al)O films over a wide range of compositions, Journal of Applied Physics 100 (2006) 07371.

[21] M. Ahmad, E. Ahmed, Y.W. Zhang, N.R. Khalid, J.F. Xu, M. Ullah, L. H. Zhang, Preparation of highly efficient Al-doped ZnO photocatalyst by combustion synthesis, Current Applied Physics (2012)http://dx.doi.org/10.1016/j.cap.2012.11.0 08.

[22] Y.H. Yan, N. Song, Z. Huang, D.B. Li, Preparation and application of nanometer ZAO powders, Materials Review 22 (2008) 73–75.

[23] K.C. Hsiao, S.C. Liao, Y.J. Chen, Synthesis, characterization and photocatalytic property of nanostructured Al-doped ZnO powders prepared by spray pyrolysis, Materials Science and Engineering: A 447 (2007) 71–76.

[24] Z.X. Yang, Y. Huang, G.N. Chen, Z.P. Guo, S.Y. Cheng, S.Z. Huang, Ethanol gas sensor based on Al-doped ZnO nanomaterial with many gas diffusing channels, Sensors and Actuators, B: Chemical 140 (2009) 549–556.

[25] K.J. Chen, T.H. Fang, F.Y. Hung, L.W. Ji, S.J. Chang, S.J. Young, Y. J. Hsiao, The crystallization and physical properties of Al-doped ZnO nanoparticles, Applied Surface Science 54 (2008) 5791–5795.

[26] R.R. Piticescu, R.M. Piticescu, C.J. Monty, Synthesis of Al-doped ZnO nanomaterials with controlled luminescence, Journal of the European Ceramic Society 26 (2006) 2979–2983.

[27] A. Louiza, H. Saliha, H. Sofiane, G. Kamel, G. Lakhder, Structural and luminescence properties of pure and Al-doped ZnO nanopowders, Materials Science and Engineering: B 177 (2012) 902–907.

[28] C.X. Luo, J.K. Liu, Y. Lu, C.S. Du, Controllable preparation and sterilization activity of zinc aluminum oxide nanoparticles, Materials Science and Engineering: C 32 (2012) 680–684.

[29] W. Shao, R.X. Ma, B. Liu, Fabrication and properties of ZAO powder, sputtering target materials and the related films, Journal of University of Science and Technology Beijing 13 (2006) 346–349.

[30] C.X. Luo, Y. Wang, J.K. Liu, J.S. Lian, C.F. Chai, Characterizations and application of conductive ZAO nanocrystals prepared by ultrasonic-template method, Acta Physico-Chimica Sinica 24 (2008) 1007–1011.

[31] Y. Huan, W. He, Z.Z. Xu, Q.T. Zhang, Preparation and properties of doped ZAO powders, Advanced Functional Materials 40 (2009) 494–497.

[32] L. Kong, X.W. Yin, L.T. Zhang, L.F. Cheng, Effect of Aluminum Doping on Microwave Absorption Properties of ZnO/$ZrSiO_4$ Composite Ceramics, Journal of the American Ceramic Society 95 (2012) 3158–3165.

[33] Y.X. Huang, Q.X. Cao, Z.M. Li, G.F. Li, Y.P. Wang, Y.G. Wei, First-principles calculation of microwave dielectric properties of Al-doping ZnO powders, Acta Physica Sinica 58 (2009) 8002–8006.

[34] A. Ahmed, Ali Ahmed, Z. Abidin Tailib, M.Z. Bin Hussein, A. Zakaria, Zn–Al laryered double hydroxide prepared at different molar ratios: preparation, characterization, optical and dielectric properties, Journal of Solid State Chemistry 191 (2012) 271–278.

[35] R.C. Wang, C.P. Liu, J.L. Huang, S.J. Chen, Singel-crystalline Al–ZnO nanowires/nanotubles synthesized at low temperature, Applied Physics Letters 88 (2006) 023111.

[36] Y.S. Rim, S.M. Kim, H.W. Choi, S.J. Park, K.H. Kim, Preparation of Al-doped ZnO thin film deposited at room temperature, Colloids and Surface A 313–314 (2008) 461–464.

[37] Y.H. Yan, Preparation ZAO Nanometer Powders by Microwave Co-Precipitation Method, Kunming University of Science and Technology, KunMing, 2008.